

Aminopeptidase-N/CD13 is a potential proapoptotic target in human myeloid tumor cells

Marion Piedfer,^{*,†,‡} Daniel Dauzonne,[§] Ruoping Tang,^{||} Juliette N'Guyen,[¶]
Christian Billard,^{*,†,‡} and Brigitte Bauvois^{*,†,‡,¶}

*Centre de Recherche des Cordeliers, Institut National de la Santé et de la Recherche Médicale (INSERM) U872, Paris, France; [†]Université Pierre et Marie Curie, Unité Mixte de Recherche en Santé (UMRS) 872, Paris, France; [‡]Université Paris-Descartes, UMRS 872, Paris, France; [§]Centre National de la Recherche Scientifique (CNRS) 176, Institut Curie, Paris, France; ^{||}Département d'Hématologie, Hôpital St. Antoine, Paris, France; and [¶]Département Maladies Infectieuses, Hôpital Cochin, Paris, France

ABSTRACT The transmembrane metalloprotease aminopeptidase-N (APN)/CD13 is overexpressed in various solid and hematological malignancies in humans, including acute myeloid leukemia (AML) and is thought to influence tumor progression. Here, we investigated the contribution of APN/CD13 to the regulation of growth and survival processes in AML cells *in vitro*. Anti-CD13 monoclonal antibodies MY7 and SJ1D1 (which do not inhibit APN activity) and WM15 (an APN-blocking antibody) inhibited the growth of the AML cell line U937 and induced apoptosis, as evidenced by cell accumulation in the sub-G₁ phase, DNA fragmentation, and phosphatidylserine externalization. Isotype-matched IgG1 and the APN/CD13 enzymatic inhibitors bestatin and 2',3-dinitroflavone-8-acetic acid, were ineffective. Internalization of CD13-MY7 complex into cells was followed by mitochondrial membrane depolarization, Bcl-2 and Mcl-1 down-regulation, Bax up-regulation, caspase-9, caspase-8, and caspase-3 activation, and cleavage of the caspase substrate PARP-1. The broad-spectrum caspase inhibitor Z-VAD-fmk and the caspase-9- and caspase-8-specific inhibitors significantly attenuated apoptosis. CD13 ligation also induced apoptosis and PARP-1 cleavage in primary AML blasts, whereas normal blood cells were not affected. Overall, these data provide new evidence that CD13 can serve as a target for inducing caspase-dependent apoptosis in AML (independently of its APN activity). These findings may have implications for tumor biology and treatment.—Piedfer, M., Dauzonne, D., Tang, R., N'Guyen, J., Billard, C., Bauvois, B. Aminopeptidase-N/CD13 is a potential proapoptotic target in human myeloid tumor cells. *FASEB J.* 25, 2831–2842 (2011). www.fasebj.org

Key Words: AML • APN • antibody • inhibitor • Bcl-2 family

AMINOPEPTIDASE-N (APN)/CD13 (EC 3.4.11.2) is a transmembrane protease present in many tissues and cell types (*e.g.*, endothelial and epithelial cells, fibroblasts, and leukocytes; ref. 1). CD13 expression is

dysregulated in inflammatory diseases and in solid and hematological tumors (1). Furthermore, CD13's enzymatic activity modulates the responses of bioactive peptides (*e.g.*, vasoactive peptides, neuropeptides, and chemokines; ref. 1). The CD13 protein is also a receptor for coronaviruses (1). Several natural and synthetic APN inhibitors have been characterized and used to reveal that CD13 can influence major biological processes, including cell growth and invasion and angiogenesis in various cellular systems (1–3). CD13's involvement in these processes has mostly been confirmed by blockage with anti-CD13 monoclonal antibodies (mAbs; refs. 2–9). However, the molecular mechanisms underlying these effects have yet to be described in detail. Indeed, it is not clear whether APN enzymatic activity is required for CD13's other functions. Some researchers have suggested that signal transduction accounts for some of CD13's functions (10–12). With regard to apoptosis, the presence of CD13 correlates with neutrophil resistance to TNF- α -induced apoptosis *via* reduced shedding of TNF-receptor I (13). Although studies with APN inhibitors have indicated a potential role for CD13 in apoptosis, this effect remains controversial because high doses of the inhibitors used might induce cytotoxicity in a nonspecific manner (1, 12).

Acute myeloid leukemia (AML) is a deadly disease characterized by the clonal expansion and accumulation of hematopoietic stem cells arrested at various stages of development. The latter are used to define distinct AML subfamilies (14–16). CD13 is strongly expressed on stem cells and leukemic blasts in all AML subtypes (1, 16). Leukemia cells are unable to undergo growth arrest, terminal differentiation, and apoptosis in response to appropriate environmental stimuli and disseminate from the bone marrow into peripheral tissues (14–16). There are no data on CD13's possible

¹ Correspondence: Centre de Recherche des Cordeliers, INSERM U872, 15 Rue de l'École de Médecine, F-75270 Paris Cedex 06, France. E-mail: brigitte.bauvois@crc.jussieu.fr
doi: 10.1096/fj.11-181396

functions in AML cells or its contribution to the course of the disease.

The recent review by Wickström *et al.* (17) on CD13 evaluates the evidence for CD13 as a target in cancer therapy. In the present study, we investigated and compared the effects of anti-CD13 mAbs and inhibitors of APN/CD13 enzymatic activity on the AML cell line U937 *in vitro* and cells from patients with AML *ex vivo*. In contrast to APN inhibitors, anti-CD13 mAbs induced growth arrest and apoptosis in AML cells. We identified some of the molecular apoptotic pathways triggered by CD13 ligation and that led to mitochondrial membrane depolarization, caspase activation, and the alteration expression of Bcl-2 family proteins known to be involved in the control of mitochondria-dependent apoptosis.

MATERIALS AND METHODS

Antibodies and reagents

Anti-CD13 (MY7, mIgG1), anti-CD13 (SJ1D1, mIgG1), phycoerythrin (PE)-conjugated anti-CD13 (SJ1D1, mIgG1), fluorescein isothiocyanate (FITC)-anti-CD14 (RM052, mIgG2a), FITC-anti-CD33 (mIgG1, D3HL60.251), and goat F(ab')₂ fragment anti-mouse fluorescein isothiocyanate-conjugated Ig (GAM-FITC) were obtained from Beckman-Coulter (Luminy, France). Anti-CD13 WM15 (mIgG1) was purchased from BD-Pharmingen (San Jose, CA, USA). The anti-CD13 mAbs were found to be endotoxin-low (<0.1 EU) in the LAL assay developed by Genscript USA (Piscataway, NJ, USA). FITC-mIgG1, FITC-mIgG2a, anti-phospho-Ser-136-Bad (Ser-136, rabbit IgG), anti-Bad (H-168, rabbit IgG), anti-PARP-1 (F-2, mIgG2a), anti-Bid (FL-195, rabbit IgG), anti-Bcl2 (100, mIgG1), and anti-Mcl-1 (S-19, rabbit IgG) were from Santa Cruz Biotechnology (Tebu-Bio, SA, France). Z-IETD-fmk (a caspase-8 inhibitor), caspase-3/-8/-9 kit assays, mIgG1 and anti-TNF- α converting enzyme (TACE; 111633, mIgG1) were obtained from R&D Systems (Abingdon, UK). Anti-actin (C4, mIgG1) was obtained from ICN Biomedicals (Aurora, OH, USA). Anti-Bax (33-6400, mIgG1) was obtained from Zymed Laboratories (San Francisco, CA, USA). Horseradish peroxidase (HRP)-conjugated secondary antibodies were purchased from GE Healthcare Europe (Saclay, France). Bestatin (hydrochloride; B8385), Ala-p-nitroanilide, etoposide, and phorbol myristoyl acetate (PMA) were obtained from Sigma (St. Louis, MO, USA). Z-VAD-fmk (a broad-spectrum caspase inhibitor), PD98059 (MEK1 inhibitor), Ly294002 (PI3K inhibitor), and AKT1/2 inhibitor VIII were from Calbiochem (Darmstadt, Germany). Ac-LEHD-CHO (a caspase-9 inhibitor) was from AG Scientific. (San Diego, CA, USA). The specific CD13/APN inhibitor 2',3-dinitroflavone-8-acetic acid (DNFAA) was synthesized as described in Bauvois *et al.* (18) and dissolved in DMSO.

Cells and treatments

The mycoplasma-free AML cell line U937 (CRL-1593.2; American Type Culture Collection, Manassas, VA, USA) with the French-American-British (FAB) phenotype M5 (19) was cultured in RPMI 1640 medium (Life Technologies, Paisley, UK) supplemented with 5% heat-inactivated FCS (Life Technologies; LPS levels < 0.1 ng/ml), 2 mM L-glutamine, 1 mM sodium pyruvate, and 40 μ g/ml gentamicin (Life Technolo-

gies) in a 5% CO₂ humidified atmosphere at 37°C. Cells were used at passage 8 or less and harvested in log-phase growth for every experiment. Cells (1–3 \times 10⁵/ml) were treated with APN inhibitors (1–100 μ M), IgG1 or anti-CD13 mAbs (1–50 μ g/ml) for various periods of time. Etoposide (1 μ M) was used as a positive control for apoptosis induction. In negative control experiments, cells were treated with the same volume of PBS containing 0.1% sodium azide and 0.5% BSA (vehicle). Caspase inhibitors and kinase inhibitors were added at the beginning of the cultures and incubated for 60 min prior to the addition of MY7.

Blood samples from healthy donors were purchased from the Etablissement Français du Sang (Hôtel-Dieu Hospital, Paris, France). Leukemic blood samples from 21 treatment-naïve AML patients (11 men and 10 women; age range 22–80) were obtained from Saint-Antoine Hospital (Tumorothèque Leucémies Saint-Antoine, ref. 579, Paris, France) after the provision of informed consent and in agreement with the Declaration of Helsinki and its revisions. Diagnosis was established according to standard clinical criteria and the FAB committee's cytological criteria. Peripheral blood mononuclear cells (PBMCs) were separated by Ficoll-Hypaque density gradient (1.077 g/ml) centrifugation. Leukemic cells were CD13⁺CD33⁺. Normal monocytes (CD13⁺CD14⁺) were isolated by adherence, as described by Bauvois *et al.* (20). Cells (10⁶/ml) were cultured in complete RPMI 1640 medium supplemented with 10% FCS.

Determination of cell growth, cell death, and cell cycle

Cell growth was evaluated by counting the number of viable cells (with diameters ranging from 9 to 14 μ m) and dead cells (diameters ranging from 4 to 9 μ m) in a Coulter Multisizer (Beckman-Coulter). Cell cycle status was determined as described by Bhardwaj *et al.* (21) and measured with a flow cytometer (Beckman-Coulter).

Flow cytometry

Intact cells were direct or indirectly immunostained with anti-CD13 mAbs and GAM-FITC, as described by Bauvois *et al.* (22). Intracellular CD13 staining was performed in permeabilized cells by using the FACS permeabilizing kit and technique developed by BD Pharmingen. Apoptosis was measured using the annexin V-FITC/propidium iodide (PI) apoptosis detection kit (Beckman-Coulter). Stained cells (4 \times 10⁴) were analyzed by flow cytometry.

DNA fragmentation

Cells were washed twice with PBS and lysed in M-PER buffer (ThermoFisher Scientific, Illkirch, France) for 60 min on ice. Lysates containing fragmented DNA were cleared by centrifugation at 10,000 g for 15 min. Supernatant samples were treated with proteinase K (500 μ g/ml) at 50°C for 2 h. Thereafter, RNase A (500 μ g/ml) was added, and the samples were incubated at 50°C for 90 min. Electrophoresis was performed in 1.8% agarose gels containing ethidium bromide, and the bands were analyzed in a densitometer (Appigen Oncor, Illkirch, France).

Assessment of mitochondrial membrane permeability

The loss of mitochondrial membrane potential (MMP) was analyzed using the mitochondrial detection kit (Biomol, Hamburg, Germany), as described previously (23). Following

mAb treatment, cells were labeled with the lipophilic fluorochrome dye JC-1. The sample's fluorescence was recorded in a Wallac Victor 2 multitask plate reader (Perkin Elmer, Norwalk, CT, USA). The depolarization of MMP is characterized by a shift from red fluorescence (FL2) to green fluorescence (FL1), *i.e.*, a reduction in the red/green fluorescence ratio.

Enzyme assays

APN activity at the surface of intact cells (2×10^6 /ml) was assayed as described by Bauvois *et al.* (18) by using Ala-p-nitroanilide (Ala-pNA; 2 mg/ml). Formation of pNA was monitored at 405 nm. Results were expressed as nanomoles of pNA formed per 30 min per 10^5 cells at 37°C. To quantify any release of soluble APN, preconditioned medium was obtained by culturing the cells (1×10^6 /ml) for 6 and 18 h at 37°C in complete RPMI without phenol red. After rapid centrifugation, the isolated cells and the culture medium were incubated with Ala-pNA in the presence or absence of the APN inhibitor DNFAA (100 μ M). Specific APN activity was determined by subtracting the amount of Ala-pNA hydrolyzed in the absence of DNFAA (100 μ M) from the amount of Ala-pNA hydrolyzed in the presence of DNFAA.

Caspase activities were assayed with specific substrates for caspase-3 (DEVD-pNA), caspase-8 (IETD-pNA), and caspase-9 (LEHD-pNA) in cell lysates (100 μ g/assay) using the caspase cellular activity assay kits (R&D Systems), according to the manufacturer's instructions. Formation of pNA was monitored at 405 nm. Comparison of the absorbance of pNA from a treated sample with control sample allows determination of the relative increase in caspase activity.

Western blot analysis

Cells were lysed in M-PER buffer (Pierce Biotechnology, Rockford, IL, USA), supplemented with protease and phos-

phatase inhibitor cocktails (Sigma). Western blot analysis was then performed, as described previously (24). Immunoblotting was performed with primary antibodies and diluted according to the manufacturer's instructions; samples were then incubated with HRP-coupled secondary antibodies. Blots were visualized by enhanced chemiluminescence (ECL; GE Healthcare Europe) and Image 1.63 software (U.S. National Institutes of Health, Bethesda, MD, USA) was used to quantify the intensity of the bands.

Data analysis

Data are presented as means \pm SD from *n* independent experiments. A 2-tailed, paired Student's *t* test was used to compare test and control groups. The threshold for statistical significance was set to $P < 0.05$.

RESULTS

MY7, WM15, and SJ1D1 anti-CD13 mAbs label CD13 expressed on AML U937 cells to a similar extent

Surface expression of CD13 on U937 cells was assessed by flow cytometry with specific mAbs against different epitopes of CD13; WM15 mAb is known to neutralize CD13's APN enzyme activity, whereas SJ1D1 and MY7 lack this inhibitory activity (25). As shown in **Fig. 1A**, all three anti-CD13 mAbs labeled surface CD13 to a similar extent. Analysis of surface APN activity showed that saturating concentrations of SJ1D1 and MY7 had no effect on APN activity, whereas WM15 reduced the activity by $44 \pm 2\%$ ($n=3$) (**Fig. 1B**). The inhibitors bestatin and DNFAA at 10 μ M also reduced APN

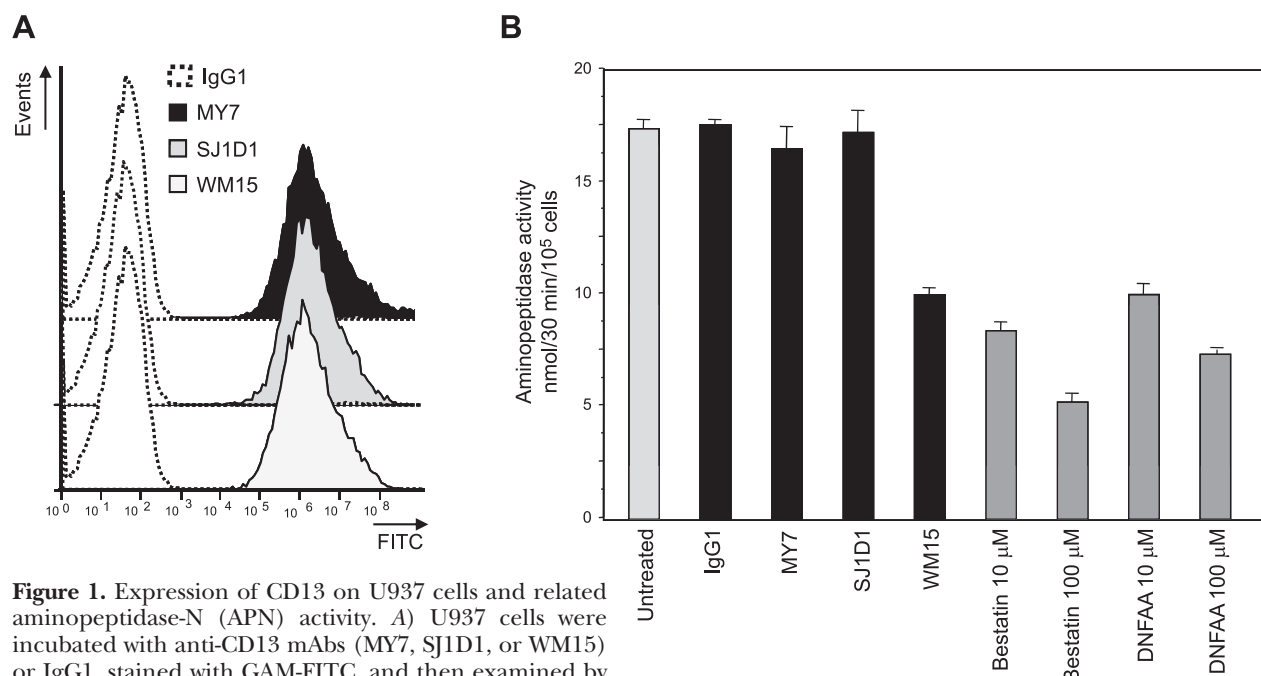


Figure 1. Expression of CD13 on U937 cells and related aminopeptidase-N (APN) activity. **A)** U937 cells were incubated with anti-CD13 mAbs (MY7, SJ1D1, or WM15) or IgG1, stained with GAM-FITC, and then examined by flow cytometry (black line). Cells treated with isotype control IgG1 served as the negative control (dotted line). **B)** Cells were assayed for APN activity using the chromogenic substrate Ala-pNA, in the absence or presence of anti-CD13 mAbs (20 μ g/ml) or the APN inhibitors bestatin and DNFAA (10 and 100 μ M in both cases), as described in Materials and Methods. Results are expressed as nanomoles of pNA formed per 30 min per 10^5 cells at 37°C. Values are expressed as means \pm SD ($n=3$).

activity to a similar extent (Fig. 1B). Residual enzyme activity was likely due to other cell surface aminopeptidases (26).

Anti-CD13 mAbs induce growth arrest and apoptosis of AML U937 cells

We next examined the effects of anti-CD13 mAbs on the growth and viability of U937 cells. Cells were cultured for 72 h in the absence or presence of increasing concentrations (1–50 $\mu\text{g}/\text{ml}$) of MY7, SJ1D1, or WM15. Cell growth was markedly reduced in anti-CD13 mAb-treated samples, when compared with isotype-matched IgG1, vehicle, or no treatment (Fig. 2A). Moreover, no effect was observed with an irrelevant mAb recognizing proteinase TACE constitutively expressed at the surface of U937 cells (Fig. 2A). The IC_{50} values were $\sim 5 \mu\text{g}/\text{ml}$ at 72 h. Kinetic studies revealed a time-dependent, inhibitory effect of anti-CD13 mAbs on U937 cell growth (Fig. 2B). Cell growth arrest was accompanied by reduction in DNA content to sub-G₁ levels (Fig. 2C for MY7; data not shown for SJ1D1 and WM15) and internucleosomal DNA fragmentation (Fig. 2D) characteristic of apoptosis. Moreover, the average diameter of dead cells ($\leq 9 \mu\text{m}$) was smaller than that of living cells. Apoptosis was further confirmed by phosphatidylser-

ine exposure at the cell surface, with consequential annexin V-FITC binding. Indeed, annexin-V binding was higher in anti-CD13 mAb-treated cells than in untreated cells or those treated with IgG1, anti-TACE, or vehicle (Fig. 3A). The proapoptotic effects of anti-CD13 mAbs were time- (Fig. 3B) and dose-dependent (Fig. 3C).

U937 cell growth and survival are not affected by the inhibition of APN/CD13 enzymatic activity

WM15 mAb was just as efficient as MY7 and SJ1D1 in strongly blocking cell growth, suggesting that CD13's active site is not involved in the inhibitory action of anti-CD13 mAbs on U937 cells. To confirm this hypothesis, we assessed the ability of APN/CD13 inhibitors to induce growth arrest and apoptosis in U937 cells. PMA (2 nM) was used as a positive control for blocking U937 cell growth (Fig. 4A). At a concentration of 100 μM , which inhibits APN activity on U937 cells (Fig. 1B), neither bestatin nor DNFAA affected the growth of U937 cells (Fig. 4A) or survival (Fig. 4B) after 96 h of treatment. These results demonstrate that the APN activity of CD13 does not contribute to anti-CD13 mAb-mediated growth arrest and apoptosis in U937 cells.

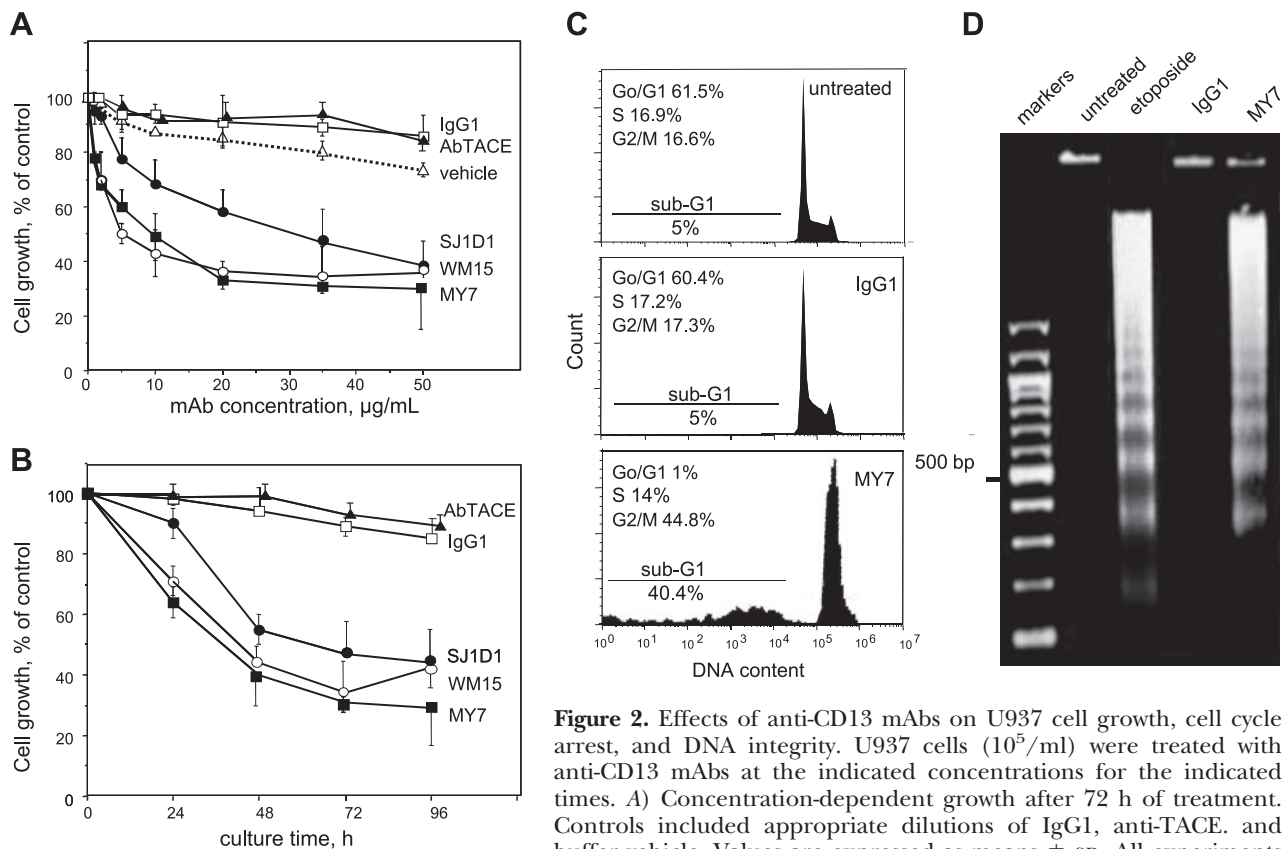


Figure 2. Effects of anti-CD13 mAbs on U937 cell growth, cell cycle arrest, and DNA integrity. U937 cells ($10^5/\text{ml}$) were treated with anti-CD13 mAbs at the indicated concentrations for the indicated times. A) Concentration-dependent growth after 72 h of treatment. Controls included appropriate dilutions of IgG1, anti-TACE, and buffer vehicle. Values are expressed as means \pm sd. All experiments were performed in duplicate and were repeated ≥ 5 times. B) Time-dependent growth with anti-CD13 mAbs (35 $\mu\text{g}/\text{mL}$). Values are expressed as means \pm sd. All experiments were performed in duplicate and were repeated ≥ 4 times. C) DNA contents of U937 cells treated for 72 h with MY7 or IgG1 (35 $\mu\text{g}/\text{mL}$) were analyzed by flow cytometry. D) DNA fragmentation U937 cells treated for 72 h with MY7 or IgG1 (35 $\mu\text{g}/\text{mL}$) or with etoposide (1 μM , positive control).

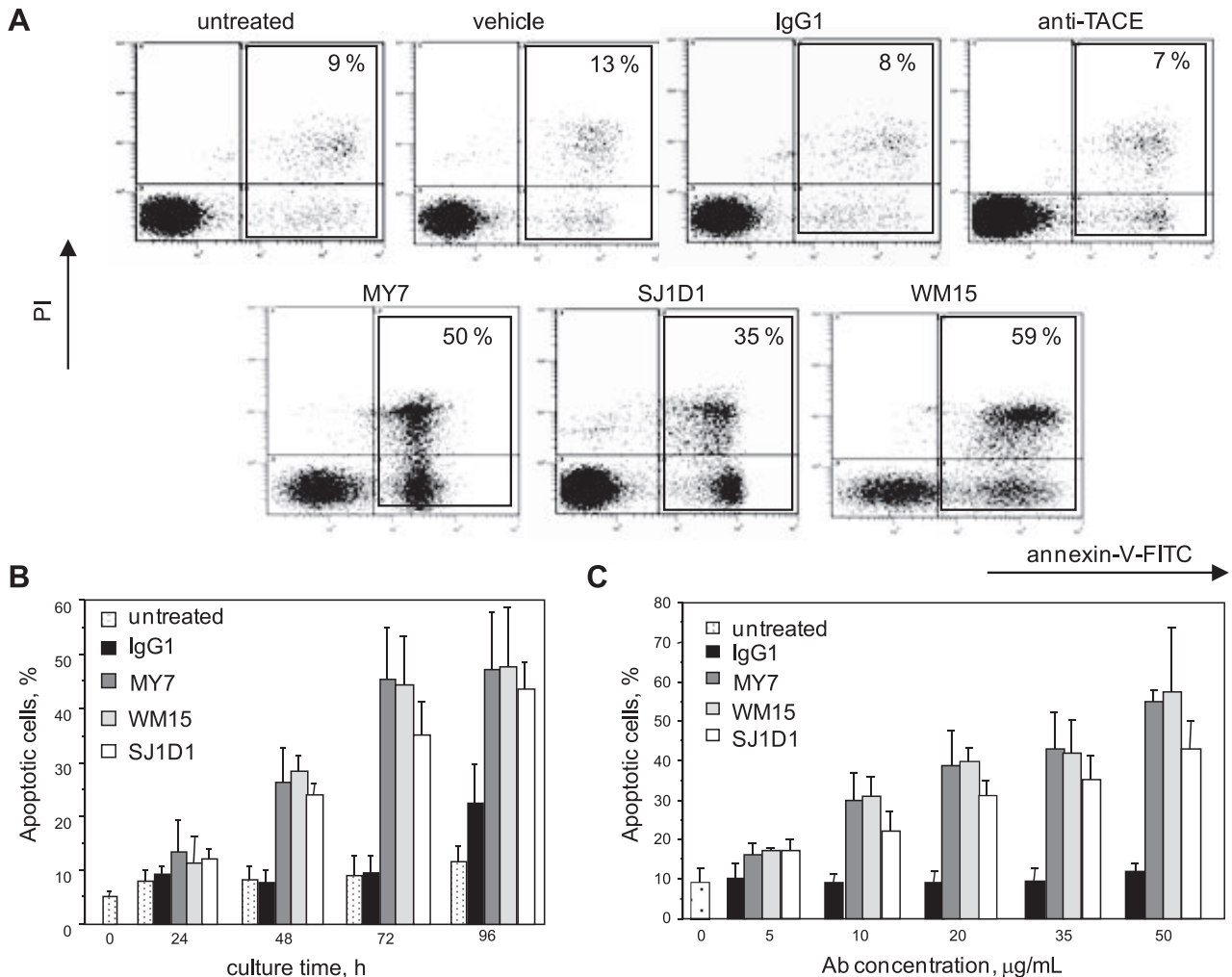


Figure 3. Anti-CD13 mAbs induce apoptosis in U937 cells. *A*) Apoptosis of U937 cells cultured for 72 h with IgG1, anti-TACE, or anti-CD13 mAbs (35 µg/ml) was evaluated by flow cytometry of FITC-conjugated annexin-V binding, while simultaneously assessing necrosis by PI staining. Results are expressed as log PI fluorescence intensity (*y* axis) *vs.* log annexin-V fluorescence intensity (*x* axis). Annexin-V-positive cells are highlighted in the box, and their percentage is shown. One representative experiment is shown. *B*) Cells were incubated for 24, 48, 72, and 96 h in the presence or absence of IgG1 or anti-CD13 mAbs (35 µg/ml), and apoptosis was assessed as described in *A*. *C*) Cells were incubated for 72 h with increasing concentrations of IgG1 or anti-CD13 mAbs (5–50 µg/ml), and apoptosis was assessed as described in *A*. Values are expressed as means ± SD. All experiments were performed in duplicate and were repeated ≥4 times.

MY7-induced internalization of surface CD13 by U937 cells

Since the internalization of cell surface receptors is thought to be a necessary step in signaling, we used flow cytometry to assess internalization of CD13 by the MY7 anti-CD13 mAb (as a decrease in CD13 surface expression). Cells were incubated with MY7 (20 µg/ml) for 6 and 18 h at 37°C. As seen in **Fig. 5A_c**, surface CD13 levels fell over time on MY7-treated cells but did not change on untreated cells (**Fig. 5A_a**) and IgG1-treated cells (**Fig. 5A_b**). Accordingly, the surface APN activity of U937 cells was specifically decreased by stimulation with MY7 (**Fig. 5B**). No significant differences in intracellular CD13 staining were observed for untreated cells and IgG1- and MY7-treated cells (data not shown). In parallel, enzymatic assays on culture medium from untreated cells and IgG1- and MY7-treated cells were

performed (*i.e.*, to check that surface CD13 down-regulation did not result from shedding into the culture medium). Nonstimulated cells released low levels of soluble APN (<10% of the total APN activity in intact cells; **Fig. 5C**). When U937 cells were activated with PMA (*i.e.*, a positive control), surface CD13 expression and activity rose (**Fig. 5A, B**). This increase was accompanied by the release of soluble APN (with a significant, 5.7-fold enhancement at 18 h; **Fig. 5C**). In contrast, the APN activity released from MY7-treated cells did not vary over time, when compared with untreated and IgG1-treated cells (**Fig. 5C**). These findings indicate that CD13 down-regulation by MY7 likely results from cell internalization of CD13-MY7 complexes.

The fact that isotype control IgG1 had no effect on U937 cells (**Fig. 1A**) strongly suggested that the Fcγ-receptor I (Fcγ-RI/CD64) on myeloid cells was not involved in the induction of apoptosis by anti-CD13

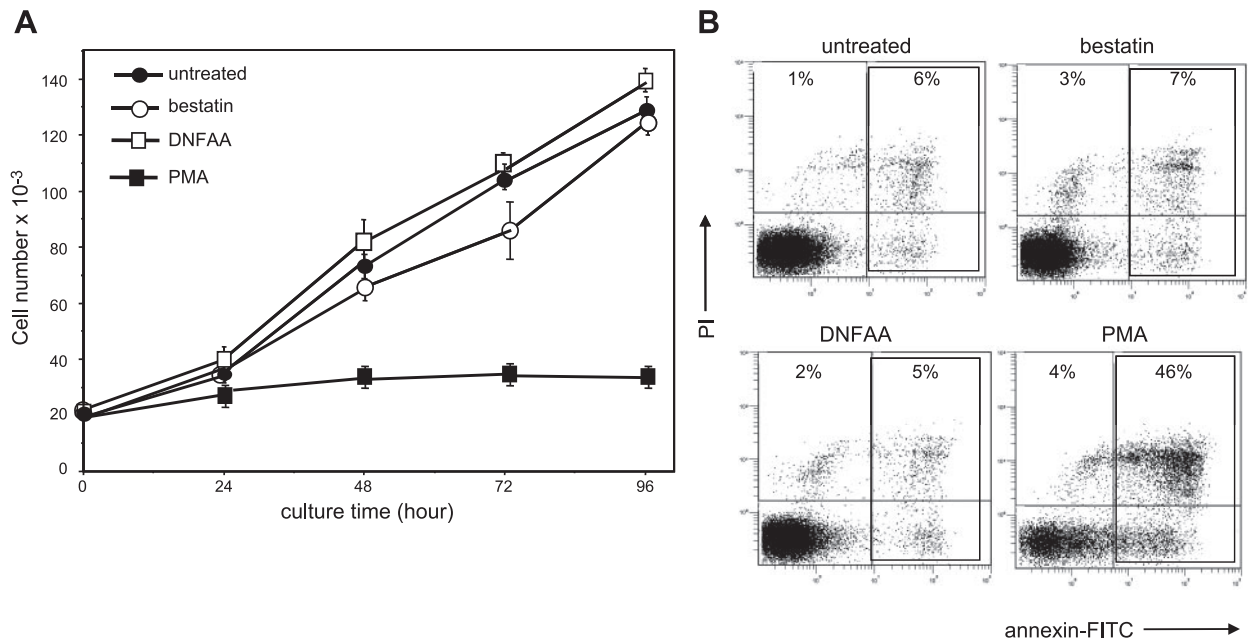


Figure 4. Effects of inhibitors of APN activity on U937 cell growth and survival. **A)** U937 cells (10^5 /ml) were treated with bestatin or DNFAA (100 μ M) or PMA (2 nM; used as positive control of growth arrest and death induction) for the indicated times. Values are means \pm sd. All experiments were performed in duplicate and were repeated 3 times. **B)** Cells (10^5 /ml) cultured for 96 h in the presence or absence of bestatin, DNFAA, or PMA, were stained with annexin-V-FITC/PI and analyzed by flow cytometry. Of note, the absence of effect was observed with 4 different batches of bestatin tested. Experiments were repeated 3 times. One representative experiment is shown. Percentage of annexin-V positive cells is shown in each box.

mAbs. U937 cells expressed detectable levels of CD64 (Fig. 5Ae), which were not affected by either IgG1 (Fig. 5Af) or MY7 (Fig. 5Ag) treatment; this observation confirmed that MY7-mediated apoptosis does not involve signaling induced by CD64 internalization.

Effects of inhibitors of PI3K, AKT, and MEK1 kinases on MY7-induced U937 cell growth arrest

PI3K/AKT and MEK signaling pathways are implicated in AML cell proliferation and survival (27, 28). We then evaluated the possible effects of PI3K, AKT, and MEK1 kinases in MY7-mediated growth arrest. PI3K inhibitor Ly294002, AKT inhibitor VIII, and MEK1 inhibitor PD98059 were used at minimally toxic concentrations, which inhibit kinase activity (29–31). U937 cells were pretreated 60 min with these inhibitors before the addition of MY7. Ly294002 (10 μ M) and AKT inhibitor VIII (2.5 μ M) significantly attenuated MY7-mediated growth arrest (Fig. 6A) and death (Fig. 6B), whereas the effect of MEK1 inhibitor (10 μ M) was marginal (Fig. 6). These results suggest the involvement of PI3K/AKT signaling in MY7-induced U937 cell growth arrest.

MY7-induced U937 cell apoptosis involves a caspase-dependent mechanism

Caspases 3, 8, and 9 are important mediators of apoptosis; caspases 8 and 9 are the initiator caspases, and caspase-3 is the “executioner enzyme” (32, 33). To establish whether caspases 3, 8, and/or 9 are activated during anti-CD13 mAb-mediated apoptosis, we studied

the ability of U937 cell lysates to cleave chromogenic substrates of these enzymes. Untreated U937 cells display similarly low baseline levels of all three caspase activities. Etoposide (1 μ M) was used as a positive control, since it triggers U937 cell death by activating these caspases (34, 35) (Fig. 7A). Kinetic studies indicated that cell treatment with MY7 (35 μ g/ml) resulted in a time-dependent increase in all three caspase activities, relative to untreated cells (Fig. 7A). Accordingly, Western blot analyses showed that exposure of U937 cells to MY7 induced the cleavage of the downstream caspase-3 substrate poly ADP-ribose polymerase-1 (PARP-1) (Fig. 7A). To determine whether the initiator caspase in the extrinsic pathway (*i.e.*, caspase-8) or the intrinsic pathway (*i.e.*, caspase-9) is involved in the apoptotic action of MY7, we examined the effects of a broad-spectrum caspase inhibitor (Z-VAD-fmk) and selective inhibitors of caspase-8 (Z-IETD-fmk) and caspase-9 (Ac-LEHD-CHO) on cell viability. MY7-induced cell death was blocked markedly by Z-VAD-fmk (85% of inhibition) and to a lesser extent by Ac-LEHD-CHO (41% of inhibition) and Z-IETD-fmk (33% of inhibition) (Fig. 7B). These results showed that MY7 induces caspase-dependent cell death through both the intrinsic and extrinsic pathways.

MY7 treatment induces mitochondrial membrane depolarization, Bax up-regulation, and Bcl-2 and Mcl-1 down-regulation

To confirm the involvement of the intrinsic pathway in MY7-induced apoptosis, we investigated the role of the

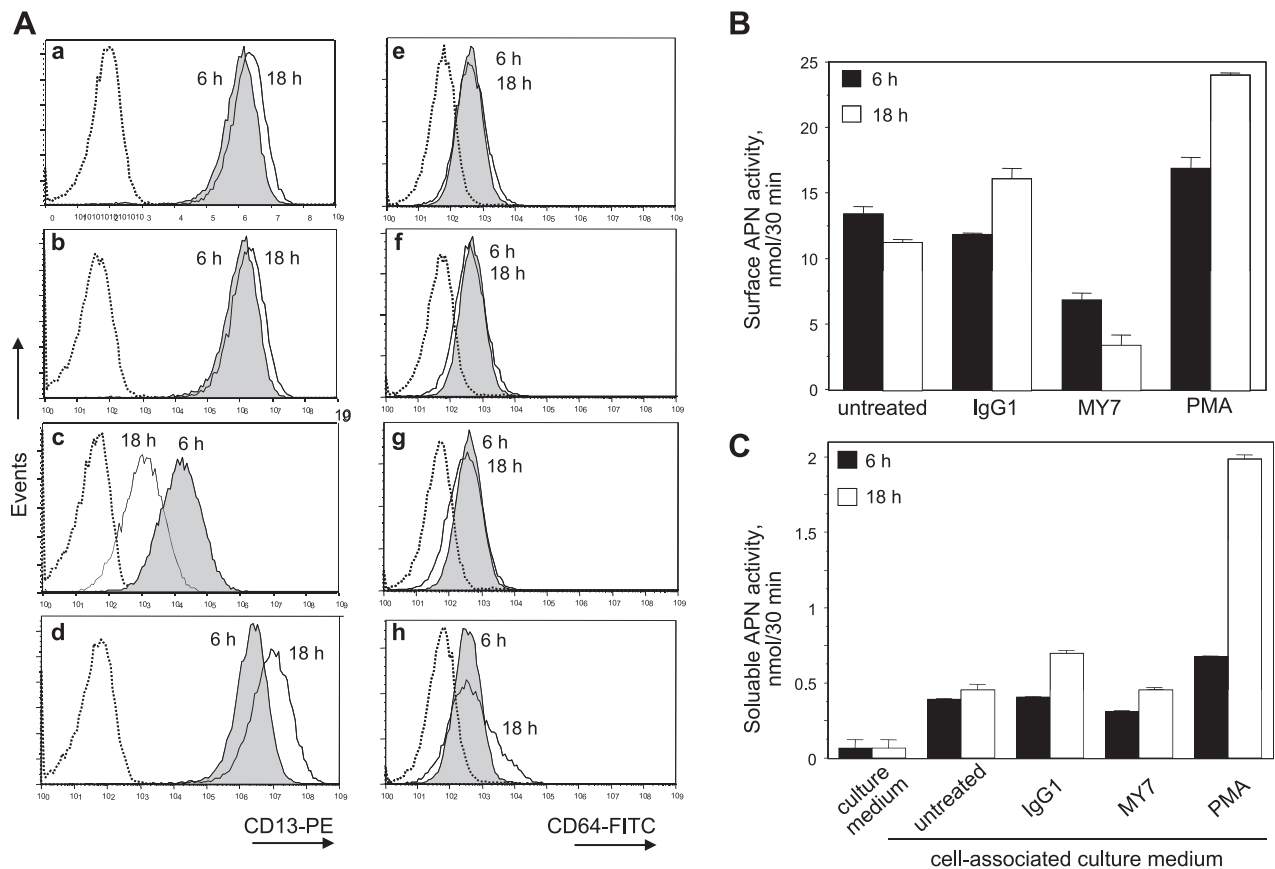


Figure 5. Effects of the anti-CD13 mAb MY7 on surface CD13 expression, surface APN activity, and soluble APN activity in U937 cells. U937 cells (10^5 /ml) were cultured for 6 and 18 h in the absence or presence of IgG1 or MY7 (20 μ g/ml) or PMA (200 nM, used as a positive control). Thereafter, the conditioned medium was collected, as described in Materials and Methods, and intact cells were assayed for CD13 expression and APN activity. *A*) Untreated cells (*a, e*) and cells treated with IgG1 (*b, f*), MY7 (*c, g*), or PMA (*d, h*) were stained with anti-CD13-PE (clone SJ1D1; *a–d*) or anti-CD64-FITC (*e–h*) and then examined by flow cytometry (black line). Cells stained with IgG1-PE and IgG1-FITC (isotype controls) served as negative controls (dotted line). *B, C*) APN activity was detected on 10^5 intact cells (*B*) and in conditioned medium (50 μ l; *C*), as described in Materials and Methods. Specific APN activity (nanomoles of pNA formed per 30 min at 37°C) was determined by subtracting the amount of pNA formed in the absence of DNFAA (100 μ M) from the amount of pNA formed in the presence of DNFAA. Values are expressed as means \pm SD ($n=3$).

mitochondria. In a fluorescence-based assay, the exposure of U937 cells to MY7 (35 μ g/ml) induced a time-dependent decrease in the MMP (Fig. 8A). Mitochondrial membrane depolarization can result from the action of proapoptotic and/or antiapoptotic mem-

bers of the Bcl-2 family (36). Therefore, we measured expression levels of Bad, Bax, and Bid proapoptotic proteins and Bcl-2 and Mcl-1 antiapoptotic proteins before and after MY7 treatment. Untreated cells expressed high levels of Bax, Bcl-2, Bid, and Mcl-1 (Fig.

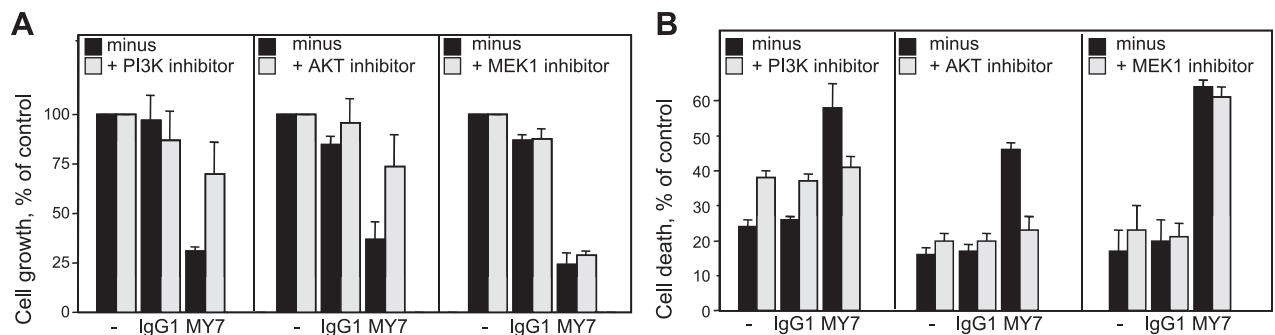


Figure 6. Effects of kinase inhibitors on MY7-induced U937 cell growth. U937 cells (10^5 /ml) were pretreated for 60 min with PI3K inhibitor Ly294002 (10 μ M), AKT1/2 inhibitor VIII (2.5 μ M), and MEK1 inhibitor PD98059 (10 μ M) and exposed to MY7 (35 μ g/ml) for 48 h. Cell growth (*A*) and cell death (*B*) were determined as described in Materials and Methods. Points represent means \pm SD of 2 independent experiments.

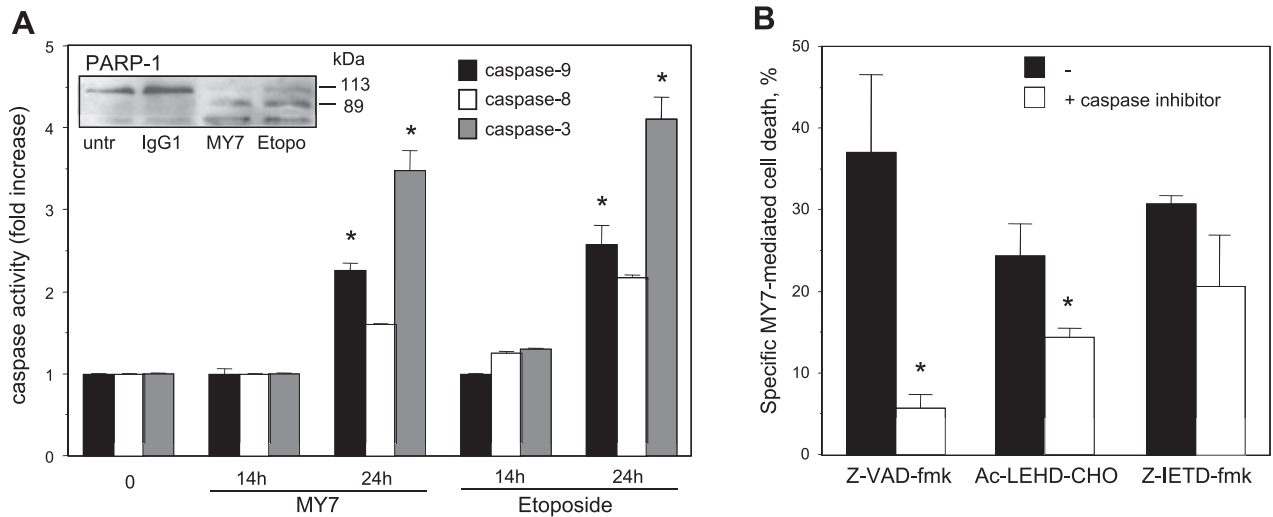


Figure 7. Anti-CD13 mAb MY7-induced apoptosis is caspase dependent. *A*) U937 cells were treated for 24 h with IgG1 or MY7 (35 $\mu\text{g/ml}$) or etoposide (1 μM) or left untreated. Caspase-3, caspase-8, and caspase-9 activities were determined using the substrates DEVD-pNA, IETD-pNA, and LEHD-pNA, respectively. Release of pNA was measured at 405 nm. Data are expressed as a fold-increase relative to the corresponding untreated samples (baseline values for caspase-3, caspase-8, and caspase-9 activity were 1.3 ± 0.2 , 2.3 ± 0.2 , and 0.9 ± 0.1 nmol pNA/60 min/100 μg protein at 37°C , respectively). Data are expressed as means \pm SD from 3 assays. IgG1 did not alter the caspase activity profile. Inset: U937 cell lysates were examined for PARP-1 expression by immunoblotting. *B*) U937 cells were incubated with IgG1 or MY7 (35 $\mu\text{g/ml}$) for 48 h after 1 h of pretreatment with Z-VAD-fmk (a broad-spectrum caspase inhibitor), Ac-LEHD-CHO (a caspase-9 inhibitor) or Z-IETD-fmk (a caspase-8 inhibitor) (50 μM). Cell death was determined as described in Materials and Methods. Percentage of specific MY7-mediated cell death was obtained by subtracting the percentage of baseline death in untreated cells or cells pretreated with caspase inhibitor from the percentage of death in the corresponding MY7-treated cells. IgG1 did not alter the baseline levels of apoptosis. Values are expressed as means \pm SD. Separate experiments were performed in duplicate and were repeated 3 times. * $P < 0.05$ vs. corresponding untreated cells.

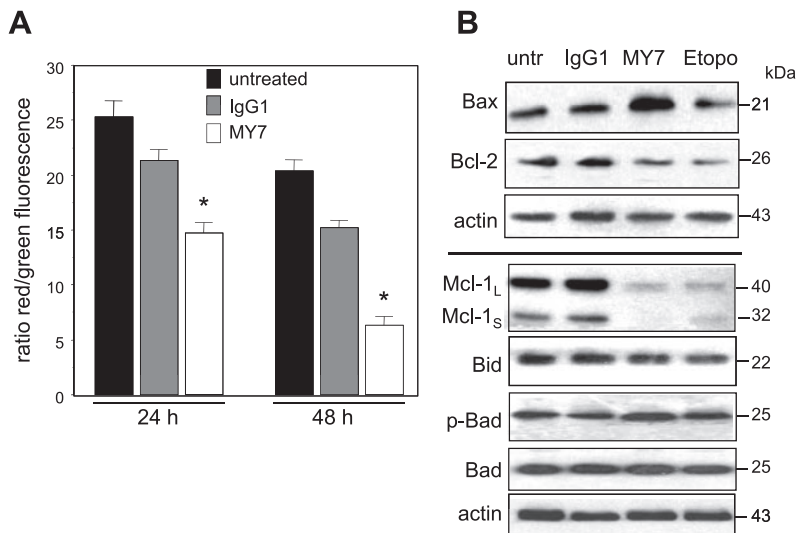
8B). No changes were observed when cells were treated with control IgG1 (Fig. 8B). Consistently with previous studies in U937 cells, Bcl-2 and Mcl-1 levels were lower in etoposide-treated cells (34, 37, 38) than in untreated cells (Fig. 8B). MY7 down-regulated Bcl-2 and Mcl-1 and up-regulated Bax (Fig. 8B). In contrast, Bid levels were not markedly affected (Fig. 8B). Dephosphorylation of Bad results in proapoptotic effects in AML (39). U937 cells were negative for Ser-112-phospho(p)-Bad (data not shown) and positive for Ser-136-p-Bad (Fig.

8B). MY7 did not alter the levels of Ser-136-p-Bad and total Bad (Fig. 8B).

Anti-CD13 mAb treatment induces apoptosis and PARP-1 cleavage in primary AML cells

Preliminary experiments had shown that the three anti-CD13 mAbs recognized similar levels of surface CD13 on primary human AML cells. To determine whether the anti-CD13 mAbs-induced apoptosis seen

Figure 8. Anti-CD13 mAb MY7 triggers dissipation of the MMP and changes in Bax, Bcl-2, and Mcl-1 expression. *A*) U937 cells were cultured for 24 and 48 h in the absence or presence of IgG1 or MY7 (35 $\mu\text{g/ml}$). Thereafter, cells were incubated for 15 min at 37°C with the fluorescent probe JC-1, washed, portioned into aliquots, and transferred in triplicate into microtiter plate wells. Green and red fluorescence were measured as detailed in Materials and Methods. Dissipation of the MMP is characterized by a significant shift in the red/green fluorescence ratio. Values are means \pm SD ($n=3$). * $P < 0.05$ vs. corresponding untreated cells. *B*) U937 cells were treated with IgG1 or MY7 (35 $\mu\text{g/ml}$) or etoposide (1 μM) for 48 h. Thereafter, lysates were Western blotted with antibodies against Bax, Bcl-2, Mcl-_L (long form), Mcl-_S (short form), Ser-136-p-Bad, Bad, Bid, and actin (a protein loading control). Two representative experiments ($n=3$ in all) are shown.



in U937 cells also occurs in primary AML blasts, we exposed PBMCs obtained from a cohort of 21 AML patients to IgG1 and to MY7 (35 $\mu\text{g}/\text{ml}$). Annexin-V binding was measured by flow cytometry after 72 h. Cultured AML cells exhibited variable baseline levels of spontaneous apoptosis (**Fig. 9A**), which were not increased by IgG1 treatment (data not shown). Exposure to MY7 increased apoptosis in 15 of 21 samples (**Fig. 9A**), and this effect was observed in all the FAB subtypes tested. In addition, MY7-responsive samples from 5 patients also responded to WM15 or SJ1D1 (data not shown). As shown in **Fig. 9B**, an increase in PARP-1 cleavage paralleled the induction of apoptosis in responders, patients 6 and 15, whereas a lack of apoptosis in nonresponders, patients 18 and 19, was associated with the same PARP profile as in untreated and IgG1-treated samples. In contrast, MY7 did not affect the viability of normal PBMCs and isolated monocytes (**Fig. 9A**).

DISCUSSION

Surface CD13 is overexpressed on human AML cells, which show abnormally high proliferation and survival. Here, we provide initial evidence that CD13 targeting

by specific anti-CD13 mAbs promotes the apoptosis of AML cells and is correlated with the ability to signal through the intertwined participation of PI3K/AKT and caspase-dependent pathways.

We examined the effects of 3 anti-CD13 mAbs (MY7, SJ1D1, and WM15, which recognize different epitopes on the leukemic CD13 antigen) on the growth and survival of AML cells. MY7 and WM15 were obtained after immunization with blasts from AML patients (25, 40), whereas SJ1D1 was raised against CD13 from the myeloid cell line KG1 (25). The epitopes on CD13 bound by SJ1D1 and MY7 are very close together. The WM15 binding site overlaps that cooccupied by SJ1D1 (25). In contrast to MY7 and SJ1D1, WM15 inhibits the APN activity of CD13 (25, 41). In the present study, we showed that all anti-CD13 mAbs recognize similar levels of surface CD13 on the AML cell line U937 (FAB M5) and on M0-, M1-, M2-, M4-, and M5-subtype primary AML cells. Following anti-CD13 mAb treatment, U937 cells undergo growth arrest and then apoptosis (as evidenced by sub- G_1 cell-cycle accumulation, DNA fragmentation, and phosphatidylserine externalization). The results in U937 cells were confirmed in primary AML cells (independently of the latter's FAB subtype), with MY7-mediated apoptosis observed in 15 of the 21 AML samples tested.

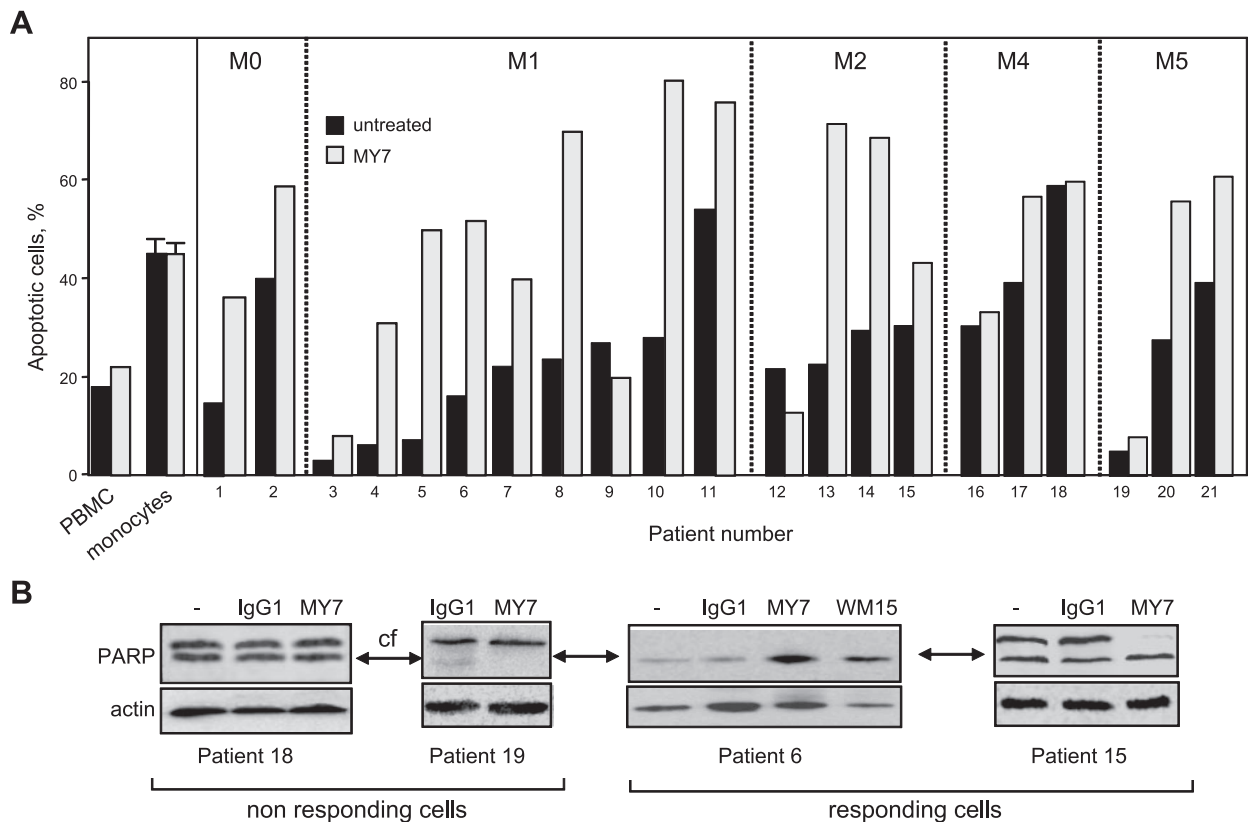


Figure 9. Anti-CD13 mAb MY7 induces apoptosis and PARP cleavage in primary AML cells. AML cells are characterized by the FAB phenotypes M5 (monoblastic), M4 (myelomonocytic), M2 (myeloblastic with maturation), M1 (myeloblastic), and M0 (undifferentiated). **A**) AML cells were cultured in the presence or absence of MY7 (35 $\mu\text{g}/\text{ml}$) for 72 h, stained with annexin-V-FITC/PI, and analyzed by flow cytometry. **B**) Cell lysates were examined for PARP or actin expression in an immunoblot assay. Arrows indicate the cleaved form (cf) of PARP. Native PARP was not detected in sample 6. Responding cells have MY7-apoptosis and PARP cleavage. Nonresponding cells lack MY7 (WM15)-apoptosis and PARP cleavage.

The APN-inhibiting WM15 mAb suppressed U937 cell growth to the same extent as the non-APN-inhibiting MY7 and SJ1D1 mAbs, suggesting that CD13's catalytic site is not involved in the inhibitory effect of anti-CD13 mAbs. Bestatin is the most frequently used CD13/APN inhibitor, although it does interact with other aminopeptidases, such as leucyl-aminopeptidase (EC 3.4.11.1) and aminopeptidase W (EC 3.4.11.16) in myeloid cells (1). In this context, we had previously synthesized a series of novel flavone-8-acetic acid derivatives and selected DNFAA as an efficient APN inhibitor (18). Bestatin and DNFAA are both slow-binding, competitive inhibitors of APN (1). When used at a concentration of 100 μ M, which inhibits APN activity (30–40 fold above the IC_{50} values), bestatin and DNFAA did not alter cell growth and survival, implying that CD13's APN activity is not required for this process. It is noteworthy that higher doses of bestatin used in previous studies might inhibit other aminopeptidase activities (1, 42). Inhibitory effects observed with high doses of bestatin ($\geq 145 \mu$ M) likely reflect bestatin intracellular effects (42).

Internalization of the CD13/anti-CD13 mAb complex suggests the existence of a signal pathway engaged by CD13. The short intracellular intracytoplasmic tail of CD13 neither contains a death domain nor a conserved immunoreceptor tyrosine-based activation motif ITAM to directly couple CD13 to intracellular effectors for inducing a cascade of events leading to cell activation. This suggests that signaling induced by the CD13/anti-CD13 mAb complex could be mediated by the physical interaction with other signaling molecules. Two studies have shown that CD13 colocalizes with Fc γ RI/CD64 on monocytes (43, 44). The receptors for the Fc portion of IgG are signaling molecules that require Syk activation. We found that isotype control IgG1 did not influence cell growth, surface CD64 was not affected by MY7 treatment, and the Syk inhibitor piceatannol did not block the proapoptotic effect of MY7. These results, therefore, indicate that Fc γ RI/CD64 does not potentiate MY7's effect on U937 cells. In U937 cells, the WM15 and SJ1D1 mAbs induced phosphorylation of ERK1/2 and p38 kinases, and inhibitors of PI3K were able to decrease their phosphorylation (45). Activated PI3K localizes to the plasma membrane and catalyzes the γ -phosphate transfer of ATP to phosphoinositides needed for phosphatidylinositol triphosphate (PIP₃) generation and calcium signaling (46). Free Ca²⁺ is reported to induce mitochondrial Ca²⁺ uptake, which can trigger mitochondrial membrane depolarization and release of cytochrome *c* and other apoptogenic proteins (47). PIP₃, in turn, activates downstream substrates, including the serine/threonine kinase AKT (46). Our data obtained with the pharmacological inhibitors of PI3K and AKT strongly suggest the implication of these kinases in the signaling cascade involved in MY7-mediated growth arrest. Anti-CD13 mAbs MY7, WM15, and Leu-M7 induced Ca²⁺ release in monocytes and U937 cells (48, 49). Furthermore, we investigated

the signaling pathways involved in the proapoptotic activity of anti-CD13 mAbs.

Apoptosis can be initiated by the mitochondrial (intrinsic) pathway and/or the death-receptor (extrinsic) pathway (33, 50). In the intrinsic apoptotic pathway, mitochondria may function as an amplifier by activating the downstream caspases 9 and 3 (33, 50). In the present study, anti-CD13 mAb treatment dissipated the mitochondrial membrane potential, activated caspase-9 and caspase-3, and cleaved PARP-1 (a major substrate of caspase-3) in U937 cells. The broad-spectrum caspase inhibitor Z-VAD-fmk and the caspase-9 inhibitor Ac-LEHD-CHO significantly attenuated MY7-mediated apoptosis, suggesting that anti-CD13 mAb treatment leads (at least) to the activation of a mitochondrial (intrinsic) caspase-dependent apoptosis pathway. Members of Bcl-2 family are important regulators of the intrinsic pathway (51). By modifying outer and inner mitochondrial membrane permeability, the Bcl-2 family (including proapoptotic Bad and Bax proteins and antiapoptotic Mcl-1 and Bcl-2 proteins) regulate cytochrome *c* release from mitochondria, caspase activation, and PARP-1 cleavage (33, 51). Overexpression of Bcl-2 protein rescues U937 cells from apoptosis (52). While Ser-136-phosphorylation of Bad protects AML cells from apoptosis (39, 53), unphosphorylated Bad can favor apoptosis by sequestering Bcl-2 within the cytoplasm and thus preventing the latter from binding to Bax; in turn, this promotes cytochrome *c* release (53, 54). Our data indicate that MY7 decreased Mcl-1 and Bcl-2 levels and increased Bax levels. However, the fact that MY7 did not affect Ser-136-p-Bad levels means that Bad is unlikely to be involved in anti-CD13-mediated apoptosis. It remains to be seen whether the inhibition of Bcl-2 and Mcl-1 by MY7 treatment is regulated at the transcriptional level or not.

In the extrinsic apoptosis pathway, triggering of death receptors (such as Fas antigen and TNF-R1) leads to strong caspase-8 activation. This bypasses mitochondria and leads directly to caspase-3 activation and then apoptosis (33, 50). However, small amounts of caspase-8 (activated by stress-induced signals within the cell) can activate the intrinsic pathway by inducing the production of truncated Bid (tBid) *via* the proteolytic cleavage of Bid (55). Following translocation from the cytosol to the mitochondrial membranes, tBid stimulates efficient oligomerization of Bax and activates the intrinsic pathway (55, 56). Our data indicate that MY7 increased caspase-8 activity in the absence of Bid cleavage and that the caspase-8 inhibitor Z-IETD-fmk, at least in part, attenuated cell death, suggesting that MY7 can also activate the extrinsic apoptosis pathway. Caspase-8 activation may be related to the extrinsic pathway, with TNF-R and/or Fas antigen triggering. In the present study, very low amounts of TNF- α (≤ 90 pg/ml/ 10^6 cells at 24 h) were detected in conditioned medium from U937 cells, and MY7 does not alter TNF- α levels (unpublished results). Moreover, cell surface expression of Fas was not significantly modified by

MY7 treatment. These data strongly suggest that anti-CD13 mAb treatment does not trigger death receptors. It remains to be seen whether anti-CD13 mAb treatment interferes with granzyme B and perforin (which can process procaspase-8) (57, 58).

In summary, we found that anti-CD13 mAbs have the ability to induce apoptosis in AML cells, related to the intertwined activation of PI3K and AKT kinases involved in signal transduction and caspases involved in the intrinsic and extrinsic pathways of apoptosis. Hence, CD13 may be a proapoptotic target in this disease. Accordingly, a recent study showed that anti-CD13 mAb WM15 was able to induce apoptosis in the HuH7 and PLC/PRF/5 human liver cancer cell lines *in vitro* (59). The anti-CD13 mAbs' ability to promote cell death might open up new interventional strategies in the treatment of CD13⁺ tumors. **[F]**

This work was funded by grants from the Institut National de la Santé et de la Recherche Médicale, the Association pour la Recherche sur le Cancer, and the Ligue contre le Cancer (Comité de Paris). The authors thank Fanny Fava for technical assistance. The authors declare no conflicting financial interests.

REFERENCES

- Bauvois, B., and Dauzonne, D. (2006) Aminopeptidase-N/CD13 (EC 3.4.11.2) inhibitors: chemistry, biological evaluations, and therapeutic prospects. *Med. Res. Rev.* **26**, 88–130
- Pasqualini, R., Koivunen, E., Kain, R., Lahdenranta, J., Sakamoto, M., Stryhn, A., Ashmun, R. A., Shapiro, L. H., Arap, W., and Ruoslahti, E. (2000) Aminopeptidase N is a receptor for tumor-homing peptides and a target for inhibiting angiogenesis. *Cancer Res.* **60**, 722–727
- Bhagwat, S. V., Lahdenranta, J., Giordano, R., Arap, W., Pasqualini, R., and Shapiro, L. H. (2001) CD13/APN is activated by angiogenic signals and is essential for capillary tube formation. *Blood* **97**, 652–659
- Saiki, I., Fujii, H., Yoneda, J., Abe, F., Nakajima, M., Tsuruo, T., and Azuma, I. (1993) Role of aminopeptidase N (CD13) in tumor-cell invasion and extracellular matrix degradation. *Int. J. Cancer* **54**, 137–143
- Ino, K., Goto, S., Okamoto, T., Nomura, S., Nawa, A., Isobe, K., Mizutani, S., and Tomoda, Y. (1994) Expression of aminopeptidase N on human choriocarcinoma cells and cell growth suppression by the inhibition of aminopeptidase N activity. *Jpn. J. Cancer Res.* **85**, 927–933
- Hashida, H., Takabayashi, A., Kanai, M., Adachi, M., Kondo, K., Kohno, N., Yamaoka, Y., and Miyake, M. (2002) Aminopeptidase N is involved in cell motility and angiogenesis: its clinical significance in human colon cancer. *Gastroenterology* **122**, 376–386
- Mina-Osorio, P., Shapiro, L. H., and Ortega, E. (2006) CD13 in cell adhesion: aminopeptidase N (CD13) mediates homotypic aggregation of monocytic cells. *J. Leukoc. Biol.* **79**, 719–730
- Mina-Osorio, P., Winnicka, B., O'Conor, C., Grant, C. L., Vogel, L. K., Rodriguez-Pinto, D., Holmes, K. V., Ortega, E., and Shapiro, L. H. (2008) CD13 is a novel mediator of monocytic/endothelial cell adhesion. *J. Leukoc. Biol.* **84**, 448–459
- Lai, A., Ghaffari, A., and Ghahary, A. (2010) Inhibitory effect of anti-aminopeptidase N/CD13 antibodies on fibroblast migration. *Mol. Cell. Biochem.* **343**, 191–199
- Lendeckel, U., Kahne, T., Riemann, D., Neubert, K., Arndt, M., and Reinhold, D. (2000) Review: the role of membrane peptidases in immune functions. *Adv. Exp. Med. Biol.* **477**, 1–24
- Breljak, D., Gabrilovac, J., and Boranic, M. (2003) Aminopeptidase N/CD13 and haematopoietic cells. *Haema* **6**, 453–461
- Mina-Osorio, P. (2008) The moonlighting enzyme CD13: old and new functions to target. *Trends Mol. Med.* **14**, 361–371
- Cowburn, A. S., Sobolewski, A., Reed, B. J., Deighton, J., Murray, J., Cadwallader, K. A., Bradley, J. R., and Chilvers, E. R. (2006) Aminopeptidase N (CD13) regulates tumor necrosis factor- α -induced apoptosis in human neutrophils. *J. Biol. Chem.* **281**, 12458–12467
- Mason, K. D., Juneja, S. K., and Szer, J. (2006) The immunophenotype of acute myeloid leukemia: is there a relationship with prognosis? *Blood Rev.* **20**, 71–82
- King, M. E., and Rowe, J. M. (2007) Recent developments in acute myelogenous leukemia therapy. *Oncologist* **12**(Suppl. 2), 14–21
- Plesa, C., Chelghoum, Y., Plesa, A., Elhamri, M., Tigaud, I., Michallet, M., Dumontet, C., and Thomas, X. (2008) Prognostic value of immunophenotyping in elderly patients with acute myeloid leukemia: a single-institution experience. *Cancer* **112**, 572–580
- Wickstrom, M., Larsson, R., Nygren, P., and Gullbo, J. (2011) Aminopeptidase N (CD13) as a target for cancer chemotherapy. *Cancer Sci.* **102**, 501–508
- Bauvois, B., Puiffe, M. L., Bongui, J. B., Paillat, S., Monneret, C., and Dauzonne, D. (2003) Synthesis and biological evaluation of novel flavone-8-acetic acid derivatives as reversible inhibitors of aminopeptidase N/CD13. *J. Med. Chem.* **46**, 3900–3913
- Fazi, F., Racanicchi, S., Zardo, G., Starnes, L. M., Mancini, M., Travaglini, L., Diverio, D., Ammatuna, E., Cimino, G., Lo-Coco, F., Grignani, F., and Nervi, C. (2007) Epigenetic silencing of the myelopoiesis regulator microRNA-223 by the AML1/ETO oncoprotein. *Cancer Cell* **12**, 457–466
- Bauvois, B., Van Weyenbergh, J., Rouillard, D., and Wietzerbin, J. (1996) TGF- β 1-stimulated adhesion of human mononuclear phagocytes to fibronectin and laminin is abolished by IFN- γ : dependence on α 5 β 1 and β 2 integrins. *Exp. Cell. Res.* **222**, 209–217
- Bhardwaj, A., Sethi, G., Vadhan-Raj, S., Bueso-Ramos, C., Takada, Y., Gaur, U., Nair, A. S., Shishodia, S., and Aggarwal, B. B. (2007) Resveratrol inhibits proliferation, induces apoptosis, and overcomes chemoresistance through down-regulation of STAT3 and nuclear factor- κ B-regulated antiapoptotic and cell survival gene products in human multiple myeloma cells. *Blood* **109**, 2293–2302
- Bauvois, B., Djavaheri-Mergny, M., Rouillard, D., Dumont, J., and Wietzerbin, J. (2000) Regulation of CD26/DPPIV gene expression by interferons and retinoic acid in tumor B cells. *Oncogene* **19**, 265–272
- Quincy, C., Billard, C., Faussat, A. M., Salanoubat, C., Ensaf, A., Nait-Si, Y., Fourneron, J. D., and Kolb, J. P. (2006) Pro-apoptotic properties of hyperforin in leukemic cells from patients with B-cell chronic lymphocytic leukemia. *Leukemia* **20**, 491–497
- Sanceau, J., Boyd, D. D., Seiki, M., and Bauvois, B. (2002) Interferons inhibit tumor necrosis factor- α -mediated matrix metalloproteinase-9 activation via interferon regulatory factor-1 binding competition with NF- κ B. *J. Biol. Chem.* **277**, 35766–35775
- Favaloro, E. J., Bradstock, K. F., Kabral, A., Grimsley, P., Zowtyj, H., and Zola, H. (1988) Further characterization of human myeloid antigens (gp160,95; gp150; gp67): investigation of epitopic heterogeneity and non-haemopoietic distribution using panels of monoclonal antibodies belonging to CD-11b, CD-13 and CD-33. *Br. J. Haematol.* **69**, 163–171
- Ashmun, R. A., and Look, A. T. (1990) Metalloprotease activity of CD13/aminopeptidase N on the surface of human myeloid cells. *Blood* **75**, 462–469
- Platanias, L. C. (2003) MAP kinase signaling pathways and hematologic malignancies. *Blood* **101**, 4667–4679
- Grandage, V. L., Gale, R. E., Linch, D. C., and Khwaja, A. (2005) PI3-kinase/Akt is constitutively active in primary acute myeloid leukaemia cells and regulates survival and chemoresistance via NF- κ B, MAP kinase and p53 pathways. *Leukemia* **19**, 586–594
- Xie, J., Qian, J., Yang, J., Wang, S., Freeman, M. E., 3rd, and Yi, Q. (2005) Critical roles of Raf/MEK/ERK and PI3K/AKT signaling and inactivation of p38 MAP kinase in the differentiation and survival of monocyte-derived immature dendritic cells. *Exp. Hematol.* **33**, 564–572
- Rahmani, M., Yu, C., Reese, E., Ahmed, W., Hirsch, K., Dent, P., and Grant, S. (2003) Inhibition of PI-3 kinase sensitizes human

- leukemic cells to histone deacetylase inhibitor-mediated apoptosis through p44/42 MAP kinase inactivation and abrogation of p21 (CIP1/WAF1) induction rather than AKT inhibition. *Oncogene* **22**, 6231–6242
31. Nguyen, J., Gogusev, J., Knapnougel, P., and Bauvois, B. (2006) Protein tyrosine kinase and p38 MAP kinase pathways are involved in stimulation of matrix metalloproteinase-9 by TNF- α in human monocytes. *Immunol. Lett.* **106**, 34–41
 32. Broker, L. E., Kruyt, F. A., and Giaccone, G. (2005) Cell death independent of caspases: a review. *Clin. Cancer Res.* **11**, 3155–3162
 33. Wang, Z. B., Liu, Y. Q., and Cui, Y. F. (2005) Pathways to caspase activation. *Cell Biol. Int.* **29**, 489–496
 34. Sun, X. M., MacFarlane, M., Zhuang, J., Wolf, B. B., Green, D. R., and Cohen, G. M. (1999) Distinct caspase cascades are initiated in receptor-mediated and chemical-induced apoptosis. *J. Biol. Chem.* **274**, 5053–5060
 35. Engels, I. H., Stepczynska, A., Stroh, C., Lauber, K., Berg, C., Schwenzer, R., Wajant, H., Janicke, R. U., Porter, A. G., Belka, C., Gregor, M., Schulze-Osthoff, K., and Wesselborg, S. (2000) Caspase-8/FLICE functions as an executioner caspase in anti-cancer drug-induced apoptosis. *Oncogene* **19**, 4563–4573
 36. Maddika, S., Ande, S. R., Panigrahi, S., Paranjothy, T., Weglarczyk, K., Zuse, A., Eshraghi, M., Manda, K. D., Wiechec, E., and Los, M. (2007) Cell survival, cell death, and cell cycle pathways are interconnected: implications for cancer therapy. *Drug Resist. Updat.* **10**, 13–29
 37. Fujita, N., and Tsuruo, T. (1998) Involvement of Bcl-2 cleavage in the acceleration of VP-16-induced U937 cell apoptosis. *Biochem. Biophys. Res. Commun.* **246**, 484–488
 38. Sordet, O., Bettaieb, A., Brucey, J. M., Eymine, B., Droin, N., Ivarsson, M., Garrido, C., and Solary, E. (1999) Selective inhibition of apoptosis by TPA-induced differentiation of U937 leukemic cells. *Cell Death Differ.* **6**, 351–361
 39. Zhao, S., Konopleva, M., Cabreira-Hansen, M., Xie, Z., Hu, W., Milella, M., Estrov, Z., Mills, G. B., and Andreeff, M. (2004) Inhibition of phosphatidylinositol 3-kinase dephosphorylates BAD and promotes apoptosis in myeloid leukemias. *Leukemia* **18**, 267–275
 40. Griffin, J. D., Ritz, J., Nadler, L. M., and Schlossman, S. F. (1981) Expression of myeloid differentiation antigens on normal and malignant myeloid cells. *J. Clin. Invest.* **68**, 932–941
 41. Favaloro, E. J. (1991) CD-13 ('gp150'; aminopeptidase-N): co-expression on endothelial and haemopoietic cells with conservation of functional activity. *Immunol. Cell. Biol.* **69**, 253–260
 42. Grujic, M., and Renko, M. (2002) Aminopeptidase inhibitors bestatin and actinonin inhibit cell proliferation of myeloma cells predominantly by intracellular interactions. *Cancer Lett.* **182**, 113–119
 43. Mina-Osorio, P., and Ortega, E. (2005) Aminopeptidase N (CD13) functionally interacts with Fc γ Rs in human monocytes. *J. Leukoc. Biol.* **77**, 1008–1017
 44. Riemann, D., Tcherkes, A., Hansen, G. H., Wulfaenger, J., Blosz, T., and Danielsen, E. M. (2005) Functional co-localization of monocytic aminopeptidase N/CD13 with the Fc γ receptors CD32 and CD64. *Biochem. Biophys. Res. Commun.* **331**, 1408–1412
 45. Santos, A. N., Langner, J., Herrmann, M., and Riemann, D. (2000) Aminopeptidase N/CD13 is directly linked to signal transduction pathways in monocytes. *Cell. Immunol.* **201**, 22–32
 46. Martelli, A. M., Nyakern, M., Tabellini, G., Bortul, R., Tazzari, P. L., Evangelisti, C., and Cocco, L. (2006) Phosphoinositide 3-kinase/Akt signaling pathway and its therapeutical implications for human acute myeloid leukemia. *Leukemia* **20**, 911–928
 47. Bernardi, P., and Rasola, A. (2007) Calcium and cell death: the mitochondrial connection. *Subcell. Biochem.* **45**, 481–506
 48. Lohn, M., Mueller, C., Thiele, K., Kahne, T., Riemann, D., and Langner, J. (1997) Aminopeptidase N-mediated signal transduction and inhibition of proliferation of human myeloid cells. *Adv. Exp. Med. Biol.* **421**, 85–91
 49. Gredmark, S., Britt, W. B., Xie, X., Lindbom, L., and Soderberg-Naucler, C. (2004) Human cytomegalovirus induces inhibition of macrophage differentiation by binding to human aminopeptidase N/CD13. *J. Immunol.* **173**, 4897–4907
 50. Scaffidi, C., Schmitz, I., Zha, J., Korsmeyer, S. J., Krammer, P. H., and Peter, M. E. (1999) Differential modulation of apoptosis sensitivity in CD95 type I and type II cells. *J. Biol. Chem.* **274**, 22532–22538
 51. Martelli, A. M., Cocco, L., Capitani, S., Miscia, S., Papa, S., and Manzoli, F. A. (2007) Nuclear phosphatidylinositol 3,4,5-trisphosphate, phosphatidylinositol 3-kinase, Akt, and PTEN: emerging key regulators of anti-apoptotic signaling and carcinogenesis. *Eur. J. Histochem.* **51** (Suppl. 1), 125–131
 52. Park, C., Jin, C. Y., Kim, G. Y., Choi, I. W., Kwon, T. K., Choi, B. T., Lee, S. J., Lee, W. H., and Choi, Y. H. (2008) Induction of apoptosis by esculetin in human leukemia U937 cells through activation of JNK and ERK. *Toxicol. Appl. Pharmacol.* **227**, 219–228
 53. Zha, J., Harada, H., Yang, E., Jockel, J., and Korsmeyer, S. J. (1996) Serine phosphorylation of death agonist BAD in response to survival factor results in binding to 14–3-3 not BCL-X(L). *Cell* **87**, 619–628
 54. Bremer, E., van Dam, G., Kroesen, B. J., de Leij, L., and Helfrich, W. (2006) Targeted induction of apoptosis for cancer therapy: current progress and prospects. *Trends Mol. Med.* **12**, 382–393
 55. Song, G., Chen, G. G., Hu, T., and Lai, P. B. (2010) Bid Stands at the crossroad of stress-response pathways. *Curr. Cancer Drug Targets* **10**, 584–592
 56. Afonina, I. S., Cullen, S. P., and Martin, S. J. (2010) Cytotoxic and non-cytotoxic roles of the CTL/NK protease granzyme B. *Immunol. Rev.* **235**, 105–116
 57. Chowdhury, I., Tharakan, B., and Bhat, G. K. (2008) Caspases—an update. *Comp. Biochem. Physiol. B Biochem. Mol. Biol.* **151**, 10–27
 58. Bulat, N., and Widmann, C. (2009) Caspase substrates and neurodegenerative diseases. *Brain Res. Bull.* **80**, 251–267
 59. Haraguchi, N., Ishii, H., Mimori, K., Tanaka, F., Ohkuma, M., Kim, H. M., Akita, H., Takiuchi, D., Hatano, H., Nagano, H., Barnard, G. F., Doki, Y., and Mori, M. (2010) CD13 is a therapeutic target in human liver cancer stem cells. *J. Clin. Invest.* **120**, 3326–3339

Received for publication February 17, 2011.

Accepted for publication April 28, 2011.